Glass phenomenology in the hard matrix model

J. Dong   V. Elser   G. Gyawali   K. Y. Jee

J. Kent-Dobias   A. Mandaiya   M. Renz

Y. Su

Laboratory of Atomic and Solid State Physics
Cornell University
Ithaca, NY 14853-2501
USA

December 17, 2019

Abstract

We introduce a new toy model for the study of glasses: the hard-matrix model (HMM). This may be viewed as a single particle moving on $SO(N)$, where there is a potential proportional to the 1-norm of the matrix. The ground states of the model are "crystals" where all matrix elements have the same magnitude. These are the Hadamard matrices when N is divisible by four. Just as finding the latter has been a difficult challenge for mathematicians, our model fails to find them upon cooling and instead shows all the behaviors that characterize physical glasses. With simulations we have located the first-order crystallization temperature, the Kauzmann temperature where the glass has the same entropy as the crystal, as well as the standard, measurement-time dependent glass transition temperature. A new feature in this glass model is a "disorder parameter" ρ_0 that is zero for any of the crystal phases and in the liquid/glass, where it is non-zero, corresponds to the density of matrix elements at the maximum in their contribution to the energy. We conclude with speculation on how a quantum extension of the HMM, with the backdrop of current work on many-body localization, might advance the understanding of glassy dynamics.

Much of statistical mechanics is the study of "toy models," minimalistic distillations of physical systems that capture particular phenomena. The simplest model of liquids, mono-disperse hard spheres, is also much used as a model of glassy behavior. In three dimensions, and when compressed rapidly, this system produces jammed structures with a reproducible packing

1

fraction [9], but without any obvious order. However, the hard sphere model falls short in exhibiting all facets of glass phenomenology. We describe these shortcomings next, and introduce an even simpler model that might better serve as a model of structural glasses.

The *hard matrix model* (HMM) is a system comprising a single orthogonal matrix $U \in \mathrm{SO}(N)$ with 1-norm energy:

$$\Phi(U) = -\sqrt{N} \sum_{ij} |U_{ij}|. \tag{1}$$

The matrix elements are not independent, but constrained much like the bond lengths and angles in a network glass. Their number, N^2, is the "volume" of the system. The constraints in the hard sphere model are considerably weaker, and allow small clusters of spheres to act independently when they occur within a low density fluctuation. In fact, it is precisely such finite sized equilibrium fluctuations that make the hard sphere system unstable to nucleating the crystal phase[1]. If analogous nucleation events/structures exist for network glasses, they are poorly understood. The hard matrix model poses this same challenge, in a far simpler mathematical setting, because it too is potentially unstable to "crystallization."

By the generalized mean inequality we know

$$\Phi(U) \geq -\sqrt{N} N \sqrt{\sum_{ij} |U_{ij}|^2} = -N^2, \tag{2}$$

where equality is attained only when the elements of U are equal in magnitude. The ground states U^* of Φ are therefore rescaled Hadamard matrices [7] $U^* = H/\sqrt{N}$, where H has only ± 1 elements, for those N where Hadamard matrices exist. By contrast, the rigorous ground state characterization of the hard sphere model, the proof of the Kepler conjecture, required a massive amount of work [6]. There is also a Hadamard matrix conjecture, which asserts that Hadamard matrices exist for all orders N divisible by four. Empirically, from explicit enumeration up to $N = 32$ [11], the number of Hadamard matrices $\#(N)$ [16] enjoys robust growth:

$$\log \#(N) \sim 0.874 \, N^{1.6}. \tag{3}$$

Ironically, for most (evenly-even) N we lack even a single example [3], the smallest open case of the conjecture being $N = 668$. It is for this reason

---

[1]The same mechanism eliminates other packing systems, *e.g.* tetrahedra, as candidate glass models.

that the hard matrix model still deserves to be called "hard." Simple physics-inspired methods, such as gradient descent on $\Phi(U)$ from random starting points, almost always fail at finding Hadamard matrices. The most successful methods for constructing these matrices [7] are algebraic in nature and require significant computation. However, because even the most productive of these are based on finding sequences of size N^1 with special properties, the estimate (3) suggests that most Hadamard matrices are avoiding discovery.

Not only are the ground states of Φ known, so are the thermodynamic equilibrium states in the limit of zero temperature. To see this, parameterize the neighborhood of a ground state $U^* = H/\sqrt{N}$ with a skew-symmetric matrix X:

$$U(X; H) = He^X/\sqrt{N}. \tag{4}$$

Expanding (1) for small X we find

$$\Phi(X; H) = -\sum_{ij} \text{sgn}(H_{ij})(H(1 + X + \frac{1}{2}X^2 + \cdots))_{ij}$$

$$= -\text{Tr}\,(H^T H(1 + X + \frac{1}{2}X^2 + \cdots))$$

$$= -N^2 + \frac{N}{2}\text{Tr}\,(X^T X) + \cdots, \tag{5}$$

that is, the potential function reduces to a diagonal quadratic form independent of the ground state Hadamard H. That the contributions to the free energy are the same for all the ground states is in contrast to the analogous situation for hard spheres, where the free energy dependence on the stacking sequence of the close-packed triangular layers was discovered only recently and required elaborate computations [13].

Thanks to the simplicity of the local potentials (5), the limit $\beta \to \infty$ of the HMM partition function

$$Z(\beta) = \int dU\, e^{-\beta\,\Phi(U)}, \tag{6}$$

can be evaluated explicitly. With the standard scale convention, the group invariant measure for small X of the parameterization (4) is

$$dU = \prod_{1 \leq i < j \leq N} \sqrt{2}\, dX_{ij}. \tag{7}$$

Since for $\beta \to \infty$ exactly the same Gaussian integral arises around each Hadamard point of $SO(N)$, we obtain

$$Z(\beta) \underset{\beta\to\infty}{\sim} \#(N)\, e^{\beta N^2} \left(\frac{2\pi}{\beta N}\right)^{N(N-1)/4} \tag{8}$$

for those N where $\#(N) > 0$.

In the absence of quantum mechanics the entropy has an arbitrary additive constant and we are free to set $S(0) = 0$. This is equivalent to working with the rescaled partition function $\overline{Z}(\beta) = Z(\beta)/Z(0)$ and defining the entropy by $S = \log \overline{Z} + \beta \langle \Phi \rangle$, where $\langle \cdot \rangle$ is the Gibbs average. Using the known volume of $\mathrm{SO}(N)$ [12],

$$Z(0) = \int dU = 2^{(N-1)(N/4+1)} \prod_{k=2}^{N} \frac{\pi^{k/2}}{\Gamma(k/2)}, \tag{9}$$

we then have an explicit expression for the HMM entropy in the low temperature limit. Taking additionally N large, as in a thermodynamic limit, we obtain the entropy per volume

$$s = \frac{1}{N^2} S \underset{N \to \infty}{\sim} -\frac{1}{4} \log \left(2\beta \sqrt{e} \right) + \frac{1}{N^2} \log \#(N). \tag{10}$$

This result looks like it might be used to address the Hadamard matrix conjecture. By integrating the HMM specific heat $c(\beta)$ in a Markov chain Monte Carlo (MCMC) simulation, starting at $\beta = 0$, it should be possible to obtain reasonable estimates of $s(\beta) - s(0) = s(\beta)$. A comparison with (10), while lacking the precision to determine $\#(N)$ outright, might still give information about its growth. As we show next, this works for small N. However, large N is inaccessible, and the Hadamard matrix conjecture remains safe, for the same reasons that make the HMM compelling as a model for glass.

Among glass models the HMM is relatively easy to simulate. We sampled the Gibbs ensemble using MCMC, with elementary transitions generated by Givens rotations applied to pairs of rows and columns of U. The range of the Givens angle is tuned, at each temperature, so the resulting acceptance rate is 50%. By defining a "sweep" of the system to be rotations attempted on all pairs of rows and columns, a single MCMC sweep is a reasonable proxy for a time step of true dynamics, since the number of actual moves per sweep scales with the number of continuous degrees of freedom.

Figure 1 shows the MCMC heat capacity per unit volume, $c = C/N^2$, for $N = 12, 16, 20$. The evidence for a first-order phase transition in the infinite system is strong. We will say the system at high temperatures is in the *liquid phase*, and at low temperatures in the *Hadamard phase*. The latter is in fact a collection of $\#(N)$ phases, each associated with a different Hadamard "crystal" ground state. At $N = 20$ we are already at the limit of being able to maintain thermal equilibrium with Givens rotations. Near the heat capacity
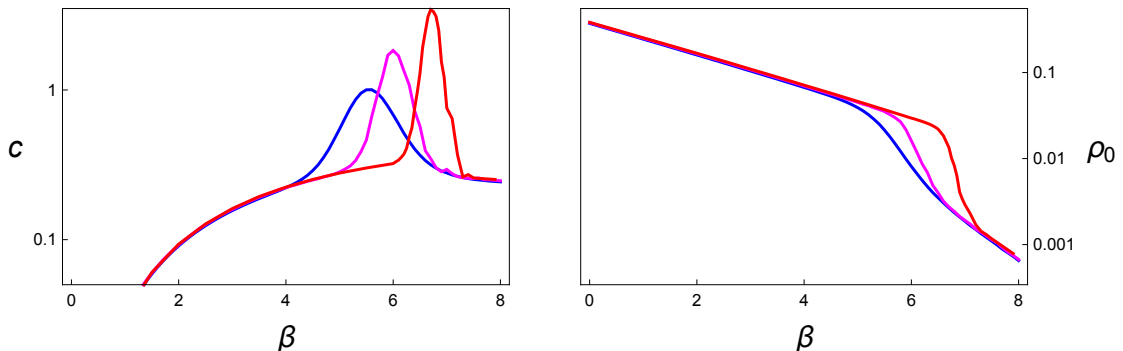
Figure 1: Equilibrium heat capacity (left) and transition state density (right) for system sizes $N = 12, 16, 20$. Narrowing of the heat capacity peak and abruptness in the drop of the associated order parameter, with increasing N, indicate a first order transition.

peak this simulation required 2×10^9 sweeps per measurement. A good test of the accuracy of the $c(\beta)$ curve is the corresponding entropy integral. When compared against (10), this reproduced the known Hadamard count $\#(20) \approx 2 \times 10^{45}$ [16] to within a factor of three[2]. The low temperature limit $c = 1/4$ is simply the equipartition value $1/2$ for quadratic potentials combined with the number of continuous modes being only half the system volume.

While all of our numerical experiments used MCMC, true dynamics could be simulated by time-evolving the unconstrained system

$$\mu N(\ddot{U} + \dot{U}\dot{U}^T U) = -\frac{1}{2}\left(\nabla\Phi - U(\nabla\Phi)^T U\right) \tag{11}$$

$$= \frac{\sqrt{N}}{2}\left(\text{sgn}(U) - U\text{sgn}(U)^T U\right), \tag{12}$$

with initial constraints

$$U(0)U^T(0) = 1, \quad \dot{U}(0)U^T(0) + U(0)\dot{U}^T(0) = 0. \tag{13}$$

The left-hand side of (11) generates free motion on $\text{SO}(N)$, and the scaling of the mass with N was chosen so the equations for small oscillation about the Hadamard minima,

$$\mu\ddot{X} = -X, \tag{14}$$

---

[2]This is before making large N approximations, as the Hadamard count makes a subextensive contribution. The counts in OEIS A206711, which include Hadamards of negative determinant, were divided by two.
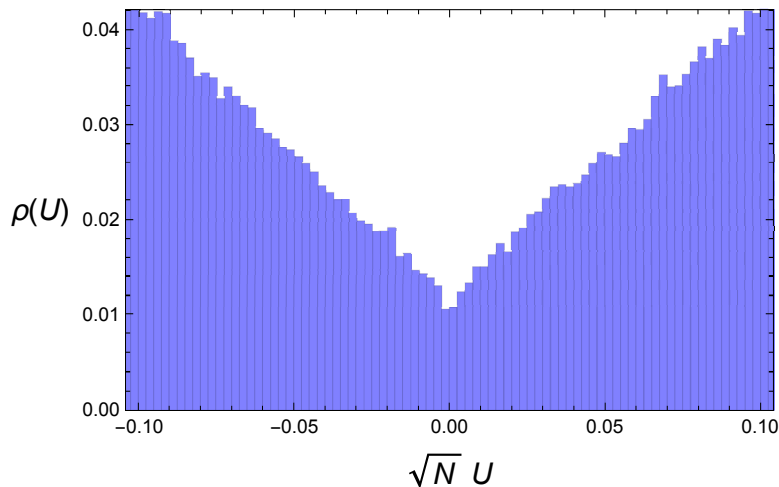
Figure 2: Detail of the distribution of matrix elements, near $U = 0$, of equilibrium points generated by gradient descent. All equilibria are fragile in the sense that some fraction of the matrix elements are near the transition point of their contribution to the energy.

are independent of N. From (12) we see that the mechanical equilibrium points of $\Phi(U)$ correspond to orthogonal matrices with the following symmetry property:

$$U^T \text{sgn}(U) = \text{sgn}(U)^T U. \tag{15}$$

These are a superset of the Hadamard matrices and it is their high abundance that defeats the prospect of finding Hadamard matrices by gradient descent on $\Phi(U)$. It is tempting to look at property (15) as a set of geometrical constraints of exactly the right number to fix all the continuous variables of an orthogonal matrix, in analogy with isostaticity in sphere packings or rigidity of ball-and-stick network models. While this perspective can be useful for identifying good glass formers when constituents are modeled geometrically [15], in our case it is simply an automatic consequence of a sufficiently well-behaved potential function.

The equilibrium points are relevant for the dynamics at low temperature. Figure 2 shows a detail of $\rho(U)$, the distribution of the individual matrix elements, near $U = 0$ where their contribution to the energy is highest. This distribution was generated by gradient descent from random points on SO(32). The property $\rho(0) > 0$, which seems to hold in the thermodynamic limit, confers a fragility to the mechanical equilibria. Consider the set of matrix elements whose values are within some fixed, small distance of zero.
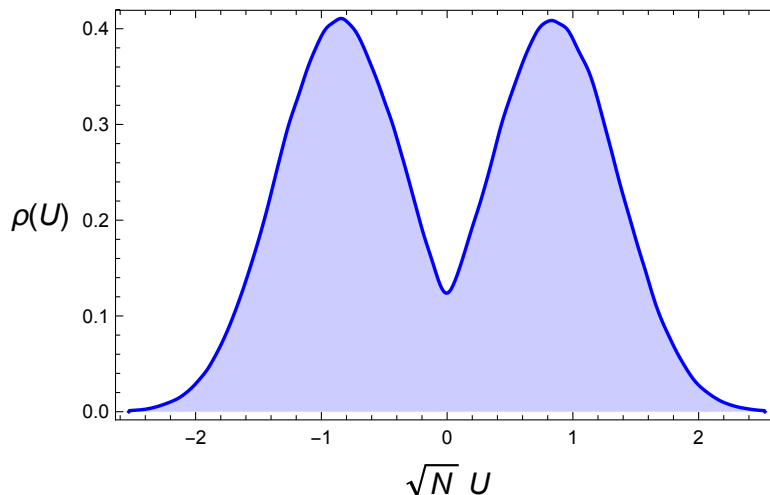
Figure 3: Probability distribution of the matrix elements at $\beta = 3$, from a $N = 32$ simulation, shows the liquid is strongly correlated well above the phase transition.

For each of these there is a small geodesic motion that brings the matrix element to the transition state point of its energy, the cusp at $U = 0$. These single-element transition states are likely also transition states for the system as a whole because the regular contribution to Φ (from the other matrix elements) only changes quadratically and the motion is small. In this restricted dynamics, called *channel flow*, the system has access to much of the low energy landscape without ever having to hop over significant barriers. On the other hand, the mixing provided by channel flow is slow because the number of continuous modes, proportional to $\rho(0)$, is small. As $\rho(0)$ decreases with temperature, equilibration becomes slower not because of rising barriers but because fewer modes are stirring the system.

The *transition state density* $\rho_0 = \rho(0)$ also serves as a (symmetry unaffiliated) "disorder parameter" of the model. As in physical glass formers, the liquid phase of the HMM is strongly correlated at temperatures well above crystallization. Whereas $\rho(U)$ is normally distributed at $\beta = 0$, we see in Figure 3 it is strongly bimodal already at $\beta = 3$. The first-order nature of the liquid/Hadamard phase transition is seen in the discontinuity-tending behavior of ρ_0, with increasing N, shown in Figure 1 for the same system sizes discussed earlier. As a disorder parameter, ρ_0 asserts a property inherent to the liquid. In being linked to dynamics via fragile equilibria and channel flow, it will also be relevant in the discussion of glasses to which we
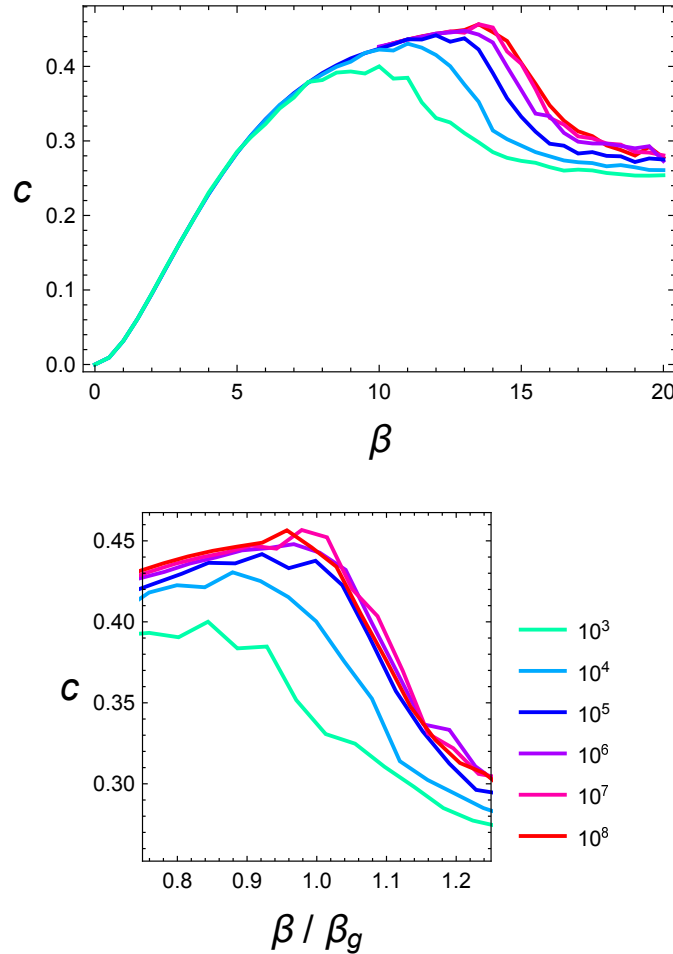
Figure 4: *Top:* Heat capacity of the $N = 32$ system with increasing number of MCMC sweeps per measurement. *Bottom:* Heat capacities replotted as a function of their reduced inverse temperature (16).

turn next.

Much of glass phenomenology [5, 4] is captured in the series of heat capacity curves shown in Figure 4 for the $N = 32$ system. These were initialized in the liquid phase and show no sign of an anomaly at the expected crystallization temperature, even at the slowest cooling rate. We estimated β_H by measuring the free energies of the metastable liquid and Hadamard phases by cooling the former and heating the latter. The free energy crossing is shown in Figure 5 and locates the transition at $\beta_H = 7.9$. Instead of a
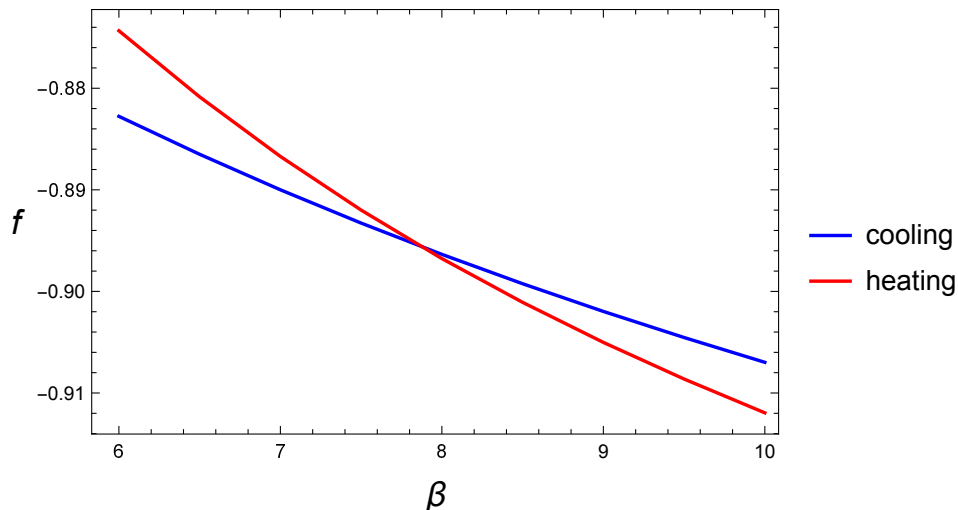
Figure 5: MCMC free energies of the $N = 32$ system cooled from the liquid and heated from one of the crystal phases.

heat capacity peak at β_H, the cooled $N = 32$ liquid exhibits a gently rising $c(\beta)$, with each reduction in cooling rate revealing slightly more of an equilibrated, metastable phase: the HMM *glass*. The equilibrium $c(\beta)$ appears to saturate at a value $c_g \approx 0.46$, about double the crystalline value of $1/4$. When the heat capacity eventually drops, close to the crystalline value, the simulation had insufficient time to sample the full range of excitations in the glass. The drop becomes more abrupt when it moves to lower temperatures with decreasing cooling rate, and the location of the drop defines β_g, the measurement-time-dependent glass transition temperature.

We will use the channel flow model, for dynamics in the glass phase, to motivate the following asymptotic form for the inverse glass transition temperature:

$$\beta_g(\tau) \sim a \log\left(b \log \tau\right). \tag{16}$$

The measurement time τ in our case is the number of MCMC sweeps (via Givens rotations tuned to have 50% acceptance rate at each temperature). When the heat capacity curves in the transition region are replotted (Figure 4, right panel) against the reduced inverse temperature, $\beta/\beta_g(\tau)$, they appear to collapse to a single curve for parameters $a = 2.3$, $b = 25$.

Our derivation of (16) hinges on the density ρ_0 of transition state matrix elements. Simulation results in the glass phase, shown in Figure 6, support
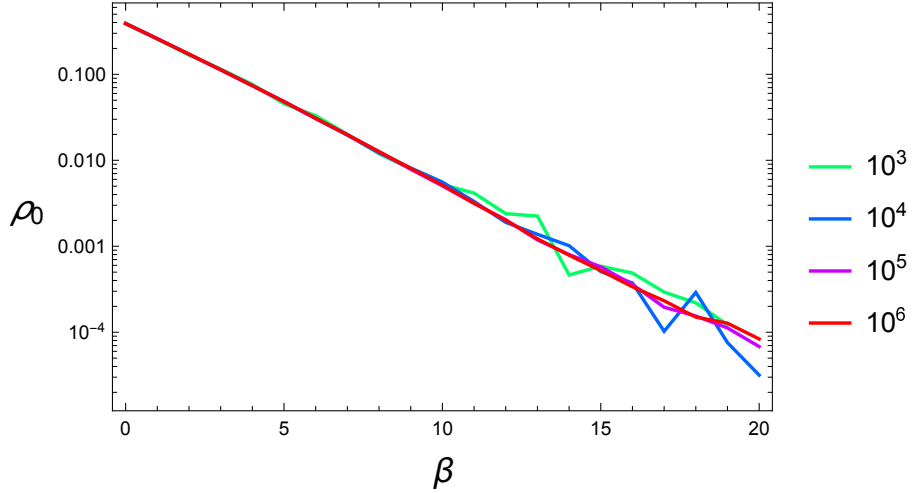
Figure 6: Density of transition state matrix elements in the glass phase of the $N = 32$ system at four cooling rates. Unlike the heat capacity (Figure 4), ρ_0 is equilibrated all the way to $\beta = 20$ with only 10^6 sweeps per measurement.

the simple thermal behavior

$$\rho_0(\beta) \propto e^{-\beta e_0}, \tag{17}$$

with $e_0 \approx 0.43$. Assuming diffusive motion for the free modes in channel flow, the characteristic distance ξ at inverse temperature β is related to the time τ by

$$\xi(\beta) \propto \tau^2. \tag{18}$$

Diffusion occurs in channels having $D(\beta)$ dimensions, and in the naive model $D(\beta)$ is simply proportional to the number of transition state matrix elements, $\rho_0(\beta)N^2$. We allow the generalization

$$D(\beta) \propto \left(\rho_0(\beta)N^2\right)^z, \tag{19}$$

where $z > 0$. For closure we assume that sampling by channel flow is not representative of the energy landscape, and thermal equilibrium is not realized, when the following volume condition holds:

$$\xi(\beta)^{D(\beta)} \ll e^{S_0}. \tag{20}$$

Here S_0 is temperature independent and represents the entropy of the space that is sampled by channel flow. This is not the same as the thermodynamic

entropy of the glass phase, which is dominated by an extensive vibrational contribution. If we interpret S_0 instead as "configurational," by (20) it would have to be sub-extensive in the case $z < 1$. For inverse temperatures below β_g, where

$$\xi(\beta_g)^{D(\beta_g)} \sim e^{S_0}, \tag{21}$$

the energy landscape is adequately sampled and channel flow manages to maintain thermodynamic equilibrium. Combining (17), (18), (19) and (21) results in the form (16) with $a = (ze_0)^{-1}$. Note that the quality of the data collapse only depends on the parameter b, while a determines which part of the collapsed curve corresponds to $\beta/\beta_g(\tau) = 1$. By the logic that time τ is required to sample the full range of energy fluctuations at inverse temperature $\beta_g(\tau)$, we determined $a \approx 2.3$ by the criterion that $\beta/\beta_g(\tau) = 1$ should correspond to the "peak" in the heat capacity for time τ. The corresponding exponent $z \approx 1$ suggests the configurational entropy of the glass is extensive. However, we stress that due to the very slow growth of $\beta_g(\tau)$ we cannot count on experiments to provide definitive evidence in favor of the form (16).

The fact that the equilibrium glass has a higher heat capacity than the crystal means that the glass entropy decreases at a higher rate with decreasing temperature [17], becoming eventually less than that of a Hadamard crystal, or even the combined entropies of all the crystals (because $\log \#(N)$ is non-extensive). From the simulated heat capacity of the slowest cooled $N = 32$ system, and assuming this stays constant at c_g at arbitrarily large β, the entropy of the glass at low temperatures is

$$s_g(\beta) = -c_g \log(\beta/\beta_0), \tag{22}$$

where $\beta_0 \approx 3.63$ comes from integrating the non-constant part of the heat capacity. Comparing (22) with (10) we find that the crystal entropy will exceed the glass entropy for $\beta > \beta_K \approx 26$.

The paradox attendant on a glass, hypothetically cooled in metastable equilibrium to β_K where it would have lower entropy than a crystal, was first brought to light by Kauzmann [10]. Brushing aside for now the possibility of diverging time scales on cooling, the paradox follows from the plausible assumptions that (i) the entropy is a sum of vibrational and configurational contributions, and (ii) the glass and crystal have nearly the same vibrational contribution. That leaves only configurational states whereby the glass can have lower entropy, but that is impossible because the crystal has zero, or at most non-extensive, configurational entropy.

Resolving the Kauzmann paradox need not hinge on exotic proposals, such as a possible thermodynamic transition to an "ideal glass" phase [17]. Conceptually, the hard sphere model is helpful in this regard. The entropy of that model, evaluated at fixed density just below the density of random close packings, gets a much larger vibrational contribution in the crystal than in the metastable random packing if "vibrational" states are estimated by the average free-volume per sphere. In the classical limit (vanishing thermal DeBroglie wavelength) the vibrational/free-volume entropy dominates any fixed configurational entropy advantage that random packings may have had. It is not paradoxical in this model that the disordered phase has the lower entropy, and in fact it is this entropic property that stabilizes the crystal, and the FCC variant in particular [13]. For the HMM, which has no system variable such as volume, the resolution of the Kauzmann paradox may be as simple as this. This model, with a continuous potential Φ, has true vibrational modes and the existence of a Kauzmann point may simply reflect the fact that the glass has stiffer phonons on average than the crystal.

To test the last hypothesis we studied the vibrations about equilibrium points U^* generated by gradient descent from low temperature Gibbs samples. Repeating the calculation (5) of the local energy, but for a general equilibrium point, we obtain

$$\Phi(X; U^*) = \Phi(U^*) + \frac{N}{2} \operatorname{Tr}(X^T K^* X) + \cdots , \tag{23}$$

where

$$K^* = \frac{1}{\sqrt{N}} U^{*T} \operatorname{sgn}(U^*) \tag{24}$$

is symmetric. Two numbers that characterize each equilibrium point are

$$\epsilon = 1 + \Phi(U^*)/N^2 \tag{25}$$

$$S_{\text{vib}} = -\log \det K^*. \tag{26}$$

Here ϵ is the energy above the Hadamard ground states and S_{vib} is proportional to the vibrational entropy, with the convention $S_{\text{vib}} = 0$ at Hadamard points because for these K^* is the identity matrix. Figure 7 shows the scatter in these numbers for three sets of 100 equilibrium points obtained by starting from Gibbs samples at $\beta = 10, 12, 14$ in the $N = 32$ system. We see that vibrational modes become stiffer at low temperature, thereby decreasing S_{vib}. Extrapolating the very linear distribution to smaller ϵ, we find $S_{\text{vib}} = 0$ for $\epsilon \approx 0.0007$. This finding casts doubt on a vibrational resolution of the Kauzmann paradox. The vibrational entropy of the glass
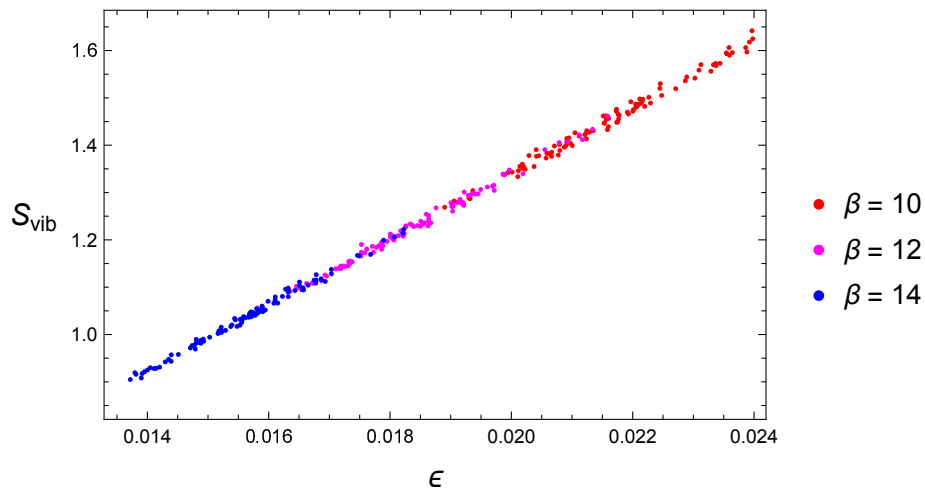
Figure 7: Distribution of excitation energy and vibrational entropy of equilibria generated by gradient descent from Gibbs samples at three temperatures.

at low temperatures should be well modeled by the vibrational entropy of the low energy equilibrium points, and this is practically indistinguishable from that of the Hadamard crystals.

To better address the Kauzmann conundrum in the HMM, while also giving a rigorous definition of states and dynamics, we introduce a quantum extension of the model. Whereas the HMM had no parameters, the Hamiltonian of the quantum model now has one:

$$\mathcal{H} = -\frac{1}{4N\mu}\Delta_U + \Phi(U). \tag{27}$$

Here Δ_U is the Laplace-Beltrami operator on $\mathrm{SO}(N)$ and the mass μ is the sole parameter. Setting the scale factor of the Laplacian so that locally ($U = e^X$, X small)

$$\Delta_U = \sum_{1 \leq i < j \leq N} \frac{\partial^2}{\partial X_{ij}^2}, \tag{28}$$

we see, using (5), that the frequency of harmonic oscillation about the Hadamard minima is $\omega = 1/\sqrt{\mu}$. At fixed β, taking the limit $\mu \to \infty$ so that $\beta(\hbar\omega) \to 0$, we recover the classical HMM which has a first-order, thermal transition at $\beta = \beta_H$. In the β-μ plane we expect this to become a line of first-order transitions. Since $\mu \to 0$ corresponds to a free particle on
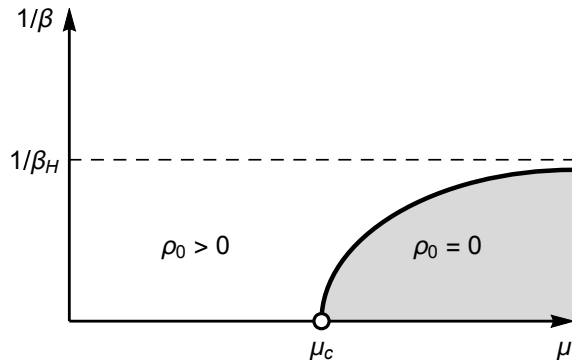
Figure 8: Conjectured phase diagram of the quantum hard matrix model.

SO(N), a model with no thermal transition, the simplest scenario for the interior of the phase diagram is that the line of first-order transitions terminates on the zero-temperature axis as sketched in Figure 8. The endpoint of the phase boundary, at $\mu = \mu_c$, would then be a quantum critical point.

The liquid and Hadamard phases acquire new interpretations when we restrict to the zero temperature axis. In the Hadamard phase the configurations (U) are localized at one of the Hadamard points of SO(N). In the limit $\mu \to \infty$ the ladder of excitations becomes more perfectly harmonic and the wavefunctions have Gaussian decay away from these points. On the other side of the quantum phase transition, $\mu < \mu_c$, the matrix U is quantum delocalized. Extending what we know about ρ_0 on the boundaries of the phase diagram into the interior, we expect $\rho_0 > 0$ everywhere in the liquid phase and $\rho_0 = 0$ everywhere under the line of first-order transitions.

We have sketched our conjectured phase diagram for the quantum model mostly to make the point that there might be a scenario for thermal equilibrium behavior without the need of an ideal glass transition. On the other hand, we also believe this phase diagram has very little physical relevance on account of glassy dynamics. We have already seen the dramatic onset of slow equilibration in MCMC simulations when using a Markov chain that mimics true dynamics. For $\beta > \beta_g$ these simulations are surely doing something like channel flow, and with a diminishing number of freely flowing modes as temperature decreases. If, as we argued above, these are tied to the value of ρ_0, then the exponential decay with β shown in Figure 6, in the glass phase, easily explains the long mixing/equilibration times in the context of classical dynamics.

The fact that the mass μ of the quantum model is a true parameter brings

the model within the scope of a very modern line of research: many-body localization (MBL) [14]. That the model has a quantum phase transition at $\mu = \mu_c$ does not seem to us as controversial. Still, asserting that for $\mu > \mu_c$ the matrices will be quantum-localized at a Hadamard point is a strange statement of the fact that it seems to be very hard to nucleate (and thereby generate) Hadamard matrices! More relevant for glassy dynamics is the behavior of the excited state wave functions with μ. If these too undergo a qualitative change, as has been observed in MBL studies on some other models without quenched disorder [8], that could explain the slow dynamics. In the channel flow picture, dynamics does not slow down because of activation over barriers, but by a diminishing number of freely flowing modes. The old-fashioned single-particle model, Anderson localization [1], now for an energy landscape on $SO(N)$, may be more relevant than MBL in this instance. There the degree of localization with energy/temperature plays a larger role than it does in MBL. What is new about the quantum-HMM, that puts it outside the scope of Anderson localization theory, is that there is no explicit randomness in the potential Φ. We suspect the localization transition, if indeed it exists, should not be sensitive to arithmetic properties of N (*e.g.* divisibility by 4) just as this plays no role in the glass phase of the classical model.

The hard matrix model also has an advantage over hard spheres for simulations in the quantum regime. In the standard path-integral scheme, updates for the quantum hard sphere model require complex world-line reconnections [2] to impose the permutation symmetry of the spheres. Updates in the quantum HMM, by contrast, can be implemented by the same bounded-range Givens rotations we used for the classical model. The only new feature in the quantum simulation is that there is a kinetic contribution,

$$\mathrm{Tr}\, U^T(\beta)\, U(\beta'), \tag{29}$$

from adjacent imaginary "times." The onset of localization, for $\mu \to \mu_c^-$, would be noticed by the behavior of the expectation value of (29), but for $|\beta - \beta'|$ that span the range of imaginary times in the simulation.

Study of the hard matrix model is also likely to advance the theory of first order phase transitions. Consider the notion of phase coexistence. We suspect that the HMM does not exhibit phase coexistence in the usual sense. Suppose the system is prepared with energy halfway between the energies of the pure phases at the transition, say by MCMC sampling at the temperature of the heat capacity peak (in a modest sized system where this is possible). What might such a system look like? We doubt that the configuration will be mixed-phase in the usual sense, say a proper Hadamard

submatrix within a "glass matrix." If such configurations existed, with continuously variable composition, then it would also be possible to have critical nuclei for crystallization, contrary to the extreme degree of metastability we observe in simulations.

The hard matrix model offers many advantages over other toy models that have been developed for the study of glasses. There are no random parameters, and the single mass parameter it does possess only sets the time scale in the classical limit of the model. Unlike hard spheres, the HMM has true vibrational modes and does not spontaneously crystallize, even for relatively small sizes. In fact, we take the absence of Hadamard constructions for most (evenly-even) N, after a century of research, as circumstantial evidence of unusually strong metastability of the HMM glass. The HMM is easy to simulate: mechanically, thermodynamically, and even quantum mechanically. Finally, the structure of the HMM glass and its dynamics is very open to examination. One product of this transparency was our channel flow model of glassy dynamics.

Acknowledgements

References

[1] P. W. Anderson. Absence of diffusion in certain random lattices. *Physical review*, 109(5):1492, 1958.

[2] D. M. Ceperley and E. Pollock. Path-integral computation of the low-temperature properties of liquid He 4. *Physical review letters*, 56(4):351, 1986.

[3] W. de Launey and D. M. Gordon. On the density of the set of known Hadamard orders. *Cryptography and Communications*, 2(2):233–246, 2010.

[4] P. G. Debenedetti and F. H. Stillinger. Supercooled liquids and the glass transition. *Nature*, 410(6825):259, 2001.

[5] M. D. Ediger, C. A. Angell, and S. R. Nagel. Supercooled liquids and glasses. *The journal of physical chemistry*, 100(31):13200–13212, 1996.

[6] T. C. Hales. A proof of the Kepler conjecture. *Annals of mathematics*, pages 1065–1185, 2005.

[7] A. Hedayat, W. D. Wallis, et al. Hadamard matrices and their applications. *The Annals of Statistics*, 6(6):1184–1238, 1978.

[8] J. M. Hickey, S. Genway, and J. P. Garrahan. Signatures of many-body localisation in a system without disorder and the relation to a glass transition. *Journal of Statistical Mechanics: Theory and Experiment*, 2016(5):054047, 2016.

[9] R. D. Kamien and A. J. Liu. Why is random close packing reproducible? *Physical review letters*, 99(15):155501, 2007.

[10] W. Kauzmann. The nature of the glassy state and the behavior of liquids at low temperatures. *Chemical reviews*, 43(2):219–256, 1948.

[11] H. Kharaghani and B. Tayfeh-Rezaie. On the classification of Hadamard matrices of order 32. *Journal of Combinatorial Designs*, 18(5):328–336, 2010.

[12] M. MacMathstein. The volume of SO(N).

[13] S.-C. Mau and D. A. Huse. Stacking entropy of hard-sphere crystals. *Physical Review E*, 59(4):4396, 1999.

[14] R. Nandkishore and D. A. Huse. Many-body localization and thermalization in quantum statistical mechanics. *Annu. Rev. Condens. Matter Phys.*, 6(1):15–38, 2015.

[15] J. C. Phillips. Topology of covalent non-crystalline solids I: Short-range order in chalcogenide alloys. *Journal of Non-Crystalline Solids*, 34(2):153–181, 1979.

[16] N. J. A. Sloane and S. Plouffe. Online Encyclopedia of Integer Sequences, https://oeis.org/A206711, 2019.

[17] F. H. Stillinger and P. G. Debenedetti. Glass transition thermodynamics and kinetics. *Annu. Rev. Condens. Matter Phys.*, 4(1):263–285, 2013.